MATHEMATICAL BIOSCIENCES
AND ENGINEERING
Volume **14**, Number **1**, February **2017**

doi:10.3934/mbe.2017018

pp. **277–287**

A CRITERION OF COLLECTIVE BEHAVIOR OF BACTERIA

Roman Czapla and Vladimir V. Mityushev*

Institute of Computer Science
Pedagogical University, ul. Podchorazych 2
Krakow 30-084, Poland

Abstract. It was established in the previous works that hydrodynamic interactions between the swimmers can lead to collective motion. Its implicit evidences were confirmed by reduction in the effective viscosity. We propose a new quantitative criterion to detect such a collective behavior. Our criterion is based on a new computationally effective RVE (representative volume element) theory based on the basic statistic moments (*e*-sums or generalized Eisenstein-Rayleigh sums). The criterion can be applied to various two-phase dispersed media (biological systems, composites etc). The locations of bacteria are modeled by short segments having a small width randomly embedded in medium without overlapping. We compute the *e*-sums of the simulated disordered sets and of the observed experimental locations of *Bacillus subtilis*. The obtained results show a difference between these two sets that demonstrates the collective motion of bacteria.

1. **Introduction.** Experimental and theoretical models have been recently developed to examine fundamental aspects of collective motion exhibited by various biological systems. Following the seminal papers [18]-[17] and works cited therein we suggest that hydrodynamic interactions between the swimmers lead to collective motion when every bacterium interacts with other ones through the viscous environment. The implicit evidences of collective motion were confirmed by reduction in the effective viscosity [16]. The theoretical investigations of collective motion were based on the considering the motion in the framework of mechanical dynamical systems [13]-[20]. While the above presented theoretical and experimental results are related via the effective viscosity of suspension of swimmers, these relation lack simple and direct comparisons of viscosity for experimentally observed sets of bacteria and for simulated ensembles.

In the present paper, we propose a new quantitative criterion of collective behavior. The locations of bacteria are modeled by short segments having a small width randomly embedded in medium without overlapping. First, we theoretically simulate locations of particles called below by *disordered sets of bacteria* (DB sets for shortness) subjected to local viscous stresses and randomly reacted on hydrodynamic interactions. Second, we calculate the basic statistic moments of the constructed DB sets in terms of the generalized Eisenstein-Rayleigh sums (*e*-sums for shortness) introduced in [6]. Further, we construct the *e*-sums (2) for the observed experimental locations (31 film frames) of *Bacillus subtilis* in a very thin liquid film

2010 *Mathematics Subject Classification.* Primary: 92B15, 92B25; Secondary: 74Q15.

Key words and phrases. Collective behavior of bacteria, disordered random sets, generalized Eisenstein-Rayleigh sums, RVE, non-overlapping segments on plane.

* Corresponding author.

[18]. As the final step, we compare the e-sums of DB sets and of the experimental locations. The obtained results show a difference between these two sets of e-sums that demonstrates the collective motion of bacteria. We do not explain reasons for the collective motion and refer to [18]-[17], [13]-[20].

Our criterion of the collective behavior is based on a new RVE (representative volume element) theory proposed in [6], on the invariance of the effective transport properties on the conformal mappings [4] and on the algebraic dependence of the viscous lattice sums on the e-sums [6]. The main object of this theory is a set of e-sums systematically investigated in [10], [8], [2], [3], [4], [15]. According to the new RVE theory, the set of the e-sums (see (2) below and general formulas in [6]) determines macroscopically equivalent cells, i.e. cells having the same effective properties (conductivity, viscosity etc). The RVE is chosen as the minimal size cell from all the equivalent cells. The necessary justification of this theory can be found in the above cited works. It is worth noting that the usage of the e-sums implicitly takes into account high order correlation functions without their hard direct computations. In particular, we make simple implementation of the RVE theory [6] which demonstrates its numerical advantages in comparison with expensive computations based on the traditional statistical notion of the RVE.

It is worth noting that the criterion can be applied to various two-phase dispersed media (biological systems, composites etc).

2. **Random location of segments.** In the present section, we discuss theoretical simulations of elements embedded in a medium. Bacteria are modeled by short segments having non-overlapping thin δ-security coatings. Random locations of segments are generated in the following way. The plane geometry is considered as the complex plane $\mathbb{C}$ of the complex variable $z = x + iy$ with standard designations accepted in complex analysis where i denotes the imaginary unit, Re and Im the real and imaginary parts, the bar stands for the complex conjugation.

The complex numbers 1 and i can be considered as the fundamental translation vectors on the complex plane $\mathbb{C}$. We introduce the $(0,0)$-cell as the square

$$Q_{(0,0)} = \left\{ z = t_1 + it_2 : -\frac{1}{2} < t_k < \frac{1}{2} \ (k = 1, 2) \right\}.$$

The square lattice $\mathcal{Q}$ consists of the cells $Q_{(m_1,m_2)} := \{z \in \mathbb{C} : z - m_1 - im_2 \in Q_{(0,0)}\}$, where m_1, m_2 run over integers.

Consider N non-overlapping segments Γ_k of length l with the centers $b_k \in Q_{(0,0)}$ with the angle of inclination $\alpha_k \in [-\pi, \pi]$. (see Fig.1).

The centers b_k are considered as random variables distributed in such a way that the segments

$$\Gamma_k = \left\{ z \in \mathbb{C} : z = b_k \pm \frac{l}{2} e^{i\alpha_k} t, \ 0 \le t \le 1 \right\}$$

generate a set of uniformly distributed non-overlapping segments. Theoretically, this distribution can be introduced as the distribution of the variable $\mathbf{b} = (b_1, b_2, \cdots, b_N) \in Q^N_{(0,0)}$ with the restrictions $|b_m - b_n| \ge \delta$ for $m \ne n$ $(m, n = 1, 2, \ldots, N)$. The separation parameter δ is taken equal to $\frac{l}{4}$. This value refers to the minimum distance between the centers of the bacteria. The choice of the constant 4 is based on the experimentally observed widths of bacteria. It should be noted that the segments Γ_k belong to the cell $Q_{(0,0)}$ in the double periodic topology when the opposite sides of $Q_{(0,0)}$ are glued by pairs.

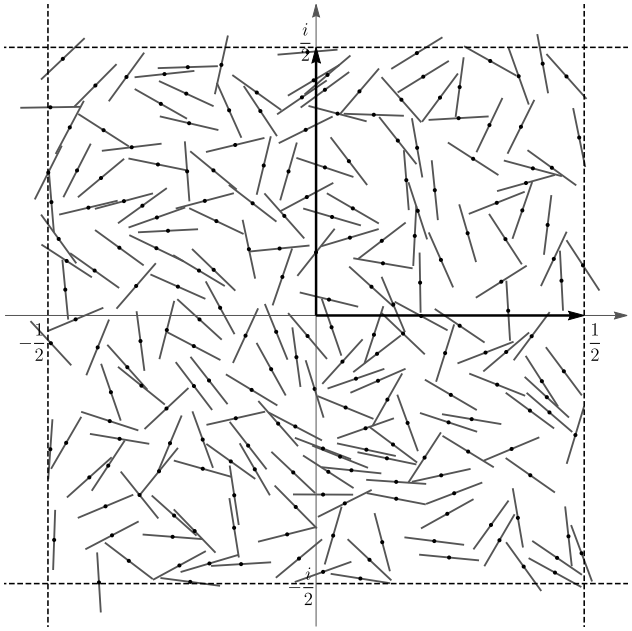

FIGURE 1. Double periodic cell $Q_{(0,0)}$ with segments.

The random variable $\mathbf{b}$ can be statistically realised for large N by the Monte Carlo method to get numerical results. The following constructive procedure to generate random locations of segments is used. Let a random point b_1 is taken in accordance with the uniform distribution in $Q_{(0,0)}$. Next, a random angle $\alpha_1 \in [-\pi, \pi]$ is chosen. Hence, the pair of points $\boldsymbol{z_1} = b_1 \pm \frac{l}{2} e^{i\alpha_1}$ is constructed. This is equivalent to the construction of the first segment Γ_1 determined by the point b_1 and angle α_1. At the next step, we take a random point b_2 uniformly distributed in $Q \backslash H_1$, where $H_1 = \{z \in \mathbb{C} \colon |z - b_1| \le \delta\}$. Further, a random angle α_2 is selected and we check whether the segments with the ends $\boldsymbol{z_2} = b_2 \pm \frac{l}{2} e^{i\alpha_2}$ and $\boldsymbol{z_1}$ do not intersect. If it is true, we have the second random segment determined by the point b_2 and angle α_2. If the segments intersect, we take a random point b_2 again in $Q \backslash H_1$ and randomly select a new random angle α_2. In the same way, we take the next point b_3 uniformly distributed in $Q \backslash (H_1 \cup H_2)$, where $H_2 = \{z \in \mathbb{C} \colon |z - b_2| \le \delta\}$ and so forth. The last random point b_N is uniformly distributed in $Q \backslash \big(\bigcup_{k=1}^{N-1} H_k \big)$ and determines a pair of points $\boldsymbol{z_N} = b_N \pm \frac{l}{2} e^{i\alpha_N}$ with the random angle α_N.

Introduce the density segments associated to the conformally invariant conductivity (capacity) [4]

$$\varrho(l, N) = N \left(\frac{l}{2} \right)^2, \tag{1}$$

where l is the length of the segment and N the number of segments per representative cell. The algorithm described above generates a probability distribution $\mathcal{U}_\varrho$ depending on the density. This distribution models the DB sets. In the limit case $\varrho = 0$, the distribution $\mathcal{U}_0$ becomes the well known Poisson distribution of points in the square.

In order to study the distributions $\mathcal{U}_\varrho$ for various densities ϱ we will use the following e-sums [9]

$$\begin{aligned} e_2 &= \frac{1}{N^2}\sum_{k=1}^{N}\sum_{m=1}^{N} E_2(b_k - b_m), \\ e_{pp} &= \frac{(-1)^p}{N^{p+1}}\sum_{m=1}^{N}\left|\sum_{k=1}^{N} E_p(b_m - b_k)\right|^2, \ p = 2,3,4. \end{aligned} \tag{2}$$

Here, E_p denotes the Eisenstein functions of order p (see Appendix). The values of the basic sums e_2, e_{22}, e_{33} and e_{44} will be estimated using the Monte Carlo method.

3. **Computation of e-sums for DB sets.** The theoretical probabilistic distributions corresponding to disordered locations of bacteria are modeled in the previous section. Now, we propose an effective computational tool to properly describe $\mathcal{U}_\varrho$.

Let M denote the number of simulated realizations of the unit cell (Monte Carlo experiments) with the random value $\boldsymbol{b}$. The parameters M and N must be chosen sufficiently large in order to obtain the stable averaged value of the e-sums. Theoretically, it is possible to consider only one experiment ($M = 1$) and to take a huge number N. But computations are less expensive if M is large and N can be not so huge as in the case $M = 1$.

First, we determine the minimal N for which the distribution is characterized in that the angles of the segments will be uniformly distributed over the interval $[-\pi, \pi]$. It is assumed that the segments directions are uniformly distributed if the following inequalities are fulfilled

$$\left|\frac{1}{N}\sum_{n=1}^{N}\mathrm{Re}\big[\exp(i\alpha_n)\big]\right| \le 0.15 \quad \text{and} \quad \left|\frac{1}{N}\sum_{n=1}^{N}\mathrm{Im}\big[\exp(i\alpha_n)\big]\right| \le 0.15, \tag{3}$$

These conditions are satisfied for $N = 500$ (see Fig.2).

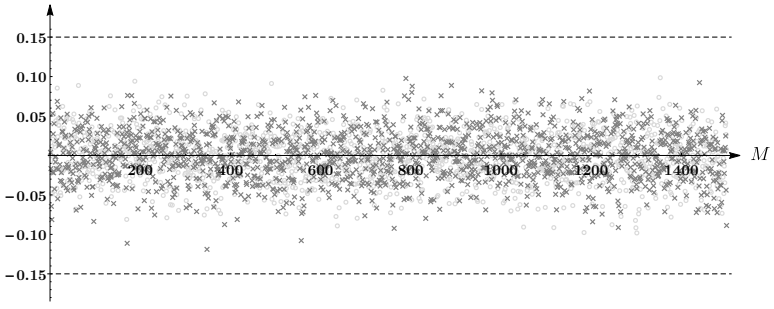

FIGURE 2. The real (circles) and imaginary (crosses) parts of the averaged directions for $N = 500$ and for the total number of distributions $M = 1500$ ($\varrho = 0.25$). All absolute values do not exceed 0.15.

In order to estimate $M_0 = M$ when the computations become stable we consider the dependence of the mean $\langle e_{44}\rangle$ on M for $M \in [1, 1500]$ experiments. All the sums e_2 and e_{pp} ($p = 2, 3, 4$) are estimated, but e_{44} is characterized by major volatility.

Here, $\langle e_{44}\rangle$ is equal to the mean value of $(e_{44})_m$ calculated for $\mathbf{b}$ generated in the m-th numerical experiment, more precisely,

$$\langle e_{44}\rangle = \frac{1}{M}\sum_{m=1}^{M}(e_{44})_m. \tag{4}$$

The results are shown in Fig.3. One can observe that errors do not exceed 2% for $M > 700$. Therefore, the computations demonstrate that we have to simulate at

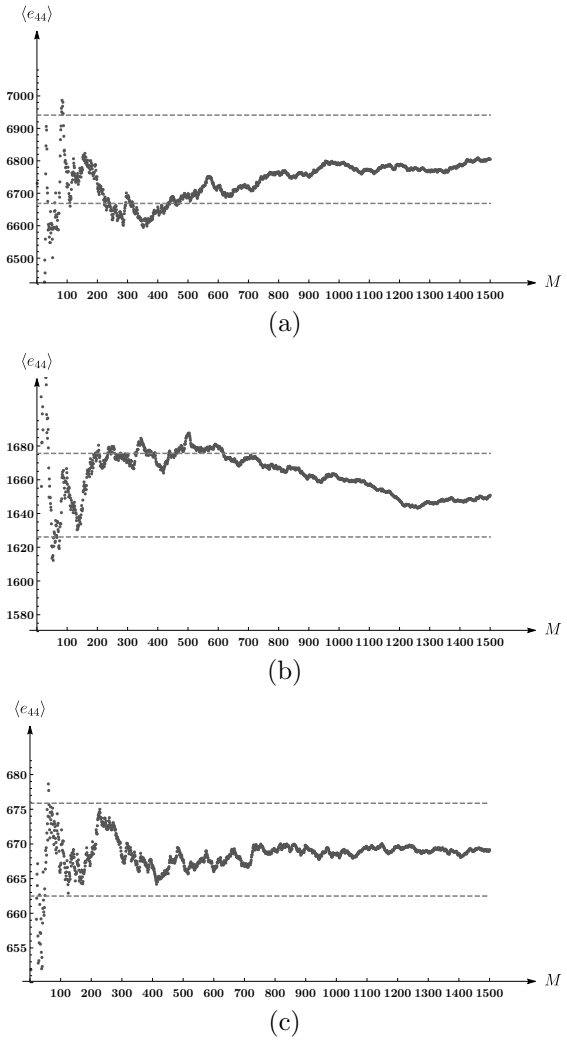

FIGURE 3. $\langle e_{44}\rangle$ for $N = 500$ and for various densities a) $\varrho = 0.15$; b) $\varrho = 0.25$; c) $\varrho = 0.35$. Dashed lines show the deviation bounds 2% (for $\varrho = 0.15$), 1.5% (for $\varrho = 0.25$) and 1% (for $\varrho = 0.35$).

least $M = 800$ cells each of them contains at least $N = 500$ segments.

The values $e_2, e_{22}, e_{33}, e_{44}$ are computed for the distributions $\mathcal{U}_\varrho$ for various densities ϱ. The sum e_2 must be equal to π [9] for ideal macroscopically isotropic random

locations of segments. This yields the first criterion equation for the macroscopic isotropy of structures. The sums e_{pp} $(p = 2, 3, 4)$ describe high order basic terms of the distributions $\mathcal{U}_\varrho$. The next terms could describe more precisely $\mathcal{U}_\varrho$ for higher densities [8].

TABLE 1. The averaged e-sums for various densities.

ϱ	$\mathrm{Re}\langle e_2 \rangle$	$\langle e_{22} \rangle$	$\langle e_{33} \rangle$	$\langle e_{44} \rangle$
0.05	3.12977	129.053	−3554.78	165787.0
0.1	3.14228	68.9110	−926.015	21743.5
0.15	**3.13271**	**48.7003**	**−424.611**	**6725.43**
0.2	3.13447	38.8351	−251.143	3037.38
0.25	3.14641	33.0394	−167.170	1635.55
0.3	3.13646	28.9718	−121.079	1000.09
0.35	3.14165	26.3229	−93.1703	672.818
0.4	3.14652	24.2258	−73.9405	472.197
0.45	3.14838	22.7573	−61.2791	354.635
0.5	3.14157	21.4983	−51.8595	274.963
0.55	3.14517	20.5061	−44.5169	218.888
0.6	3.13946	19.7609	−39.4423	180.827

The average e-sums are selected in Table 1 for the densities ϱ changing from 0.05 to 0.6 with the step 0.05. The algorithm works too slowly for higher densities. The results from Table 1 can be extended by expensive computations to higher densities.

Table 1 contains the fundamental parameters of the uniform non-overlapping distribution $\mathcal{U}_\varrho$ of segments on the plane. The simulated theoretical distribution describes DB sets when bacteria may affect each other but these interactions are local and do not yield the collective behavior.

4. **Collective motion of bacteria.** In the present section, we pay attention to experimental results partially presented in [18]. The images of *Bacillus subtilis* in 31 frames are used in computations. One of the typical frame is displayed in Fig.4.

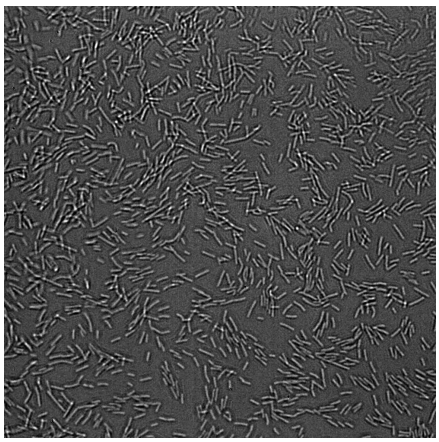

FIGURE 4. *Bacillus subtilis* [18].

We use algorithms of image processing and analysis to determine number, centers, angles of inclinations and length of bacteria. The density of bacteria is calculated by formula (1) and oscillates around value 0.15. The results of the image processing and analysis are applied to computation of the values of the experimental e-sums. The results are selected in Table 2.

TABLE 2. The e-sums for 31 film frames of *Bacillus subtilis*. The first column contains the number of the film frame, the second column contains the number of bacteria N detected in the frame. The next columns show basic sums.

$no.$	N	$\mathrm{Re}[e_2]$	e_{22}	e_{33}	e_{44}
1	2065	3.24113	35.3172	−166.312	2351.56
2	2067	3.25984	36.6725	−158.136	1920.47
3	2066	3.19667	34.8162	−164.29	2071.58
4	2040	3.29149	35.4505	−149.94	2060.21
5	2064	3.27662	33.9367	−141.591	1627.76
6	2056	3.42917	37.4054	−190.248	2867.12
7	2026	3.34495	35.6335	−157.051	1811.85
8	2030	3.13718	34.0681	−169.746	2077.70
9	2039	3.21947	34.6973	−148.317	1675.23
10	2044	3.06423	37.2784	−177.122	2865.54
11	2023	2.95417	32.9400	−157.421	1695.34
12	2014	3.09097	36.1141	−208.578	2967.78
13	2027	3.00734	36.0749	−215.528	3292.64
14	2034	3.16291	35.3946	−194.029	2697.51
15	2059	3.21142	35.7572	−175.982	2647.37
16	2016	3.19012	36.9914	−200.469	3200.68
17	2016	3.30939	35.3018	−163.073	1911.99
18	2057	3.22744	38.7036	−243.944	4057.40
19	2055	3.18527	35.9201	−144.187	1701.75
20	2071	3.31315	37.6613	−152.177	2094.90
21	2066	3.2770	33.6304	−131.371	1735.46
22	2073	3.3854	35.1252	−129.436	1330.40
23	2040	3.24423	33.6249	−126.809	1305.79
24	2080	3.30177	36.0663	−159.988	1707.04
25	2077	3.19037	34.2243	−168.806	1970.43
26	2065	3.39291	39.0489	−186.748	2108.54
27	2062	3.17936	34.0767	−138.028	1354.70
28	2024	3.11102	40.2420	−202.873	3966.32
29	2068	3.12904	33.4322	−155.213	1801.78
30	2059	3.28145	36.8591	−176.772	2198.46
31	2042	3.24301	37.0932	−208.055	2844.27

In order to compare the distributions of DB sets with the distribution of bacteria we have made theoretical calculation of 31 samples. Because of the average number of bacteria in the frame is about 2050, the minimum distance between the centers of the bacteria is $\frac{1}{4}$ of their length and density of bacteria equals about 0.15, the theoretical calculations have been carried out for the following parameters $N =$

2050, $\varrho = 0.15$ and $\delta = \frac{l}{4}$. The length $l = 0.017108$ is normalized to the normalized unit area of the cell. The results of the calculations are shown in Table 3.

TABLE 3. The e-sums calculated for 31 samples of DB sets. The parameters of distribution are $N = 2050$, $\varrho = 0.15$ and $\delta = \frac{l}{4}$.

no.	$\mathrm{Re}[\boldsymbol{e_2}]$	$\boldsymbol{e_{22}}$	$\boldsymbol{e_{33}}$	$\boldsymbol{e_{44}}$
1	3.17987	46.6427	−393.453	6565.85
2	3.07985	50.6260	−515.407	9617.15
3	3.36286	58.2470	−629.653	11184.9
4	3.31838	47.8645	−380.243	5763.63
5	3.01309	47.7780	−435.587	6984.50
6	3.14305	47.8691	−400.298	6207.25
7	3.20741	50.5550	−433.739	6256.86
8	3.20946	45.6877	−348.511	4868.42
9	3.08756	50.2205	−485.495	8630.89
10	3.14825	51.9186	−498.135	7884.83
11	3.15232	50.4770	−407.538	5794.05
12	2.97260	48.3467	−415.332	6423.79
13	3.18407	48.6382	−406.544	6317.61
14	3.12623	43.5618	−332.846	5012.32
15	2.96333	47.0048	−403.513	6158.98
16	3.13992	49.2681	−428.006	6764.48
17	3.16460	48.0914	−402.791	6347.72
18	3.09493	53.3020	−483.722	7700.97
19	3.12330	50.4108	−415.444	6743.15
20	3.21182	49.3165	−410.478	6876.66
21	3.21308	50.4445	−476.521	8126.50
22	2.97221	48.6954	−441.899	7384.68
23	3.23927	51.1514	−466.984	6864.76
24	3.11142	43.8766	−362.591	5776.80
25	2.84798	44.1550	−383.563	5705.14
26	3.09189	44.8430	−373.888	6020.28
27	3.11219	44.5645	−331.345	4733.94
28	3.05673	50.1022	−490.807	8516.17
29	3.09775	48.5431	−416.398	6597.56
30	2.99318	47.1511	−432.571	6636.21
31	3.01481	47.5799	−400.869	6078.16

5. **Conclusion.** Comparing the results shown in the Tables 2 and 3 for the observed and theoretical distributions of bacteria, we can see that values of the corresponding e-sums differ. Therefore, the observed locations of bacteria are not fitted with the simulated disordered locations. We can conclude that the behavior of the bacteria is not disordered, hence, we suggest that it is collective. An exception is the values of e_2 which is close to $\pi \approx 3.14$ for the DB sets and the observed locations (see Table 4). This demonstrates averaged isotropy of the bacteria motion for the considered data.

In order to see that the theoretical and observed distributions are essentially different, we compare averaged basic sums (see Table 4) from Table 2 and Table 3.

TABLE 4. Comparison of the averaged e-sums for the observed bacteria locations with the e-sums computed for the DB sets ($\varrho = 0.15$) from Table 2 and Table 3.

	$\mathrm{Re}[\langle \boldsymbol{e_2} \rangle]$	$\langle \boldsymbol{e_{22}} \rangle$	$\langle \boldsymbol{e_{33}} \rangle$	$\langle \boldsymbol{e_{44}} \rangle$
averaged e-sums for theoretical distributions	3.11721	48.6107	−425.941	6791.75
standard deviation of the e-sums for theoretical distributions	0.107542	3.02546	60.3803	1366.42
averaged e-sums for distributions of bacteria	3.22092	35.7922	−169.75	2255.47
standard deviation of the e-sums for distributions of bacteria	0.108139	1.73937	27.9609	717.895

It is worth noting that changes of the parameters (δ, M etc) do not essentially impact onto deviations of the e-sums of DB sets. Moreover, the DB sets have significantly higher values e_{pp} ($p = 2, 3, 4$) than the observed ones (c.f., the bold line in Table 1 and the averaged data from Table 4).

The above analysis of collective behavior can be considered as the first application of the RVE theory [6] which will be extended in the future. In particular, we plan to study dynamical parameters of the bacteria distributions in time using the data displayed in Fig.5.

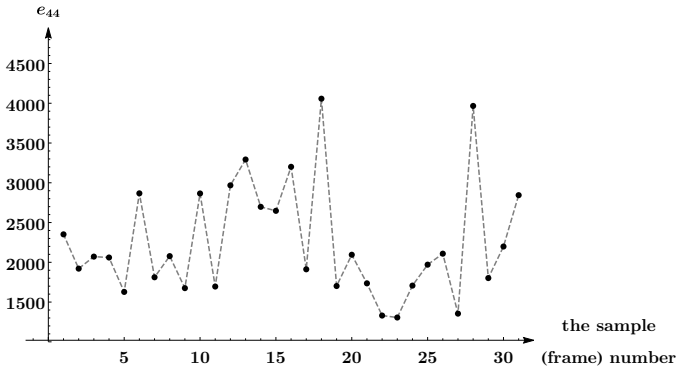

FIGURE 5. The values of e_{44} for subsequent frames of the film.

Appendix. Following [6], [7] we present constructive formulae for the Eisenstain-Rayleigh sums S_m the Eisenstain functions E_m corresponding to square lattice $\mathcal{Q}$ (see section 2).

The Eisenstein–Rayleigh lattice sums S_m can be easily calculated through the rapidly convergent series (43) and recurrent formulae (44) from paper [7]. For the

square array, we have $S_2 = \pi = 3.14159$, $S_4 = 3.15121$, $S_8 = 4.25577$, $S_{12} = 3.93885$. Only the sums S_m ($m = 2$; $m = 4, 8, 12, 16, \ldots$) do not vanish for the square array.

The Eisenstein functions [21] are related to the Weierstrass function $\wp(z)$ [1] by the identities

$$E_2(z) = \wp(z) + S_2,$$
$$E_m(z) = \frac{(-1)^m}{(m-1)!}\frac{d^{m-2}\wp(z)}{dz^{m-2}}, \quad m = 3, 4, \ldots. \tag{5}$$

Every function (5) is doubly periodic and has a pole of order m at $z = 0$. For shortness, it is convenient to redefine the Eisenstein functions in (2) at zero as $E_p(b_k - b_m) := S_p$ for $k = m$.

Acknowledgments. We thank Alexei Sokolov who kindly presented the experimental results partially reported in [18] and Leonid Berlyand for stimulated discussion during his visit to Kraków and VM's visits to Penn State University.

The authors thank the anonymous reviewer for valuable comments and suggestions to improve the paper.

REFERENCES

[1] N. I. Akhiezer, *Elements of Theory of Elliptic Functions*, Nauka, 1970 (in Russian); Engl. transl. AMS, 1990.

[2] R. Czapla, V. V. Mityushev and W. Nawalaniec, Effective conductivity of random two–dimensional composites with circular non–overlapping inclusions, *Computational Materials Science*, 63 (2012), 118–126.

[3] R. Czapla, V. V. Mityushev and W. Nawalaniec, Simulation of representative volume elements for random 2D composites with circular non-overlapping inclusions, *Theoretical and Applied Informatics*, **24** (2012), 227–242.

[4] R. Czapla, V. V. Mityushev and N. Rylko, Conformal mapping of circular multiply connected domains onto segment domains, *Electron. Trans. Numer. Anal.,* **39** (2012), 286–297.

[5] S. Gluzman, D. A. Karpeev and L. V. Berlyand, Effective viscosity of puller-like microswimmers: A renormalization approach, *J. R. Soc. Interface*, **10** (2013), 1–10.

[6] V. V. Mityushev, Representative cell in mechanics of composites and generalized Eisenstein–Rayleigh sums, *Complex Variables*, **51** (2006), 1033–1045.

[7] V. V. Mityushev and P. Adler, Longitudial permeability of a doubly periodic rectangular array of circular cylinders, *I, ZAMM (Journal of Applied Mathematics and Mechanics)*, **82** (2002), 335–345.

[8] V. V. Mityushev and W. Nawalaniec, Basic sums and their random dynamic changes in description of microstructure of 2D composites, *Computational Materials Science*, **97** (2015), 64–74.

[9] V. V. Mityushev and N. Rylko, Optimal distribution of the non-overlapping conducting disks, *Multiscale Model. Simul.*, **10** (2012), 180–190.

[10] W. Nawalaniec, Algorithms for computing symbolic representations of basic esums and their application to composites, *Journal of Symbolic Computation*, **74** (2016), 328-345.

[11] M. Potomkin, V. Gyrya, I. Aranson and L. Berlyand, Collision of microswimmers in viscous fluid, *Physical Review E*, **87** (2013), 053005.

[12] S. D. Ryan, L. Berlyand, B. M. Haines and D. A. Karpeev, A kinetic model for semi-dilute bacterial suspensions, *Multiscale Model. Simul.*, **11** (2013), 1176–1196.

[13] S. D. Rayn, B. M. Haines, L. Berlyand, F. Ziebert and I. S. Aranson, Viscosity of bacterial suspensions: Hydrodynamic interactions and self-induced noise, *Rapid Communication to Phys. Rev. E*, **83** (2011), 050904(R).

[14] S. D. Ryan, A. Sokolov, L. Berlyand and I. S. Aranson, Correlation properties of collective motion in bacterial suspensions, *New Journal of Physics*, **15** (2013), 105021, 18pp.

[15] N. Rylko, Representative volume element in 2D for disks and in 3D for balls, *J. Mechanics of Materials and Structures*, **9** (2014), 427–439.

[16] A. Sokolov and I. S. Aranson, Reduction of viscosity in suspension of swimming bacteria, *Phys. Rev. Lett.*, **103** (2009), 148101.
[17] A. Sokolov and I. S. Aranson, Physical properties of collective motion in suspensions of bacteria, *Phys. Rev. Lett.*, **109** (2012), 248109.
[18] A. Sokolov, I. S. Aranson, J. O. Kessler and R. E. Goldstein, Concentration dependence of the collective dynamics of swimming bacteria, *Physical Review Letters*, **98** (2007), 158102.
[19] A. Sokolov, R. E. Goldstein, F. I. Feldstein and I. S. Aranson, Enhanced mixing and spatial instability in concentrated bacteria suspensions, *Phys. Rev.E,* **80** (2009), 031903.
[20] M. Tournus, L. V. Berlyand, A. Kirshtein and I. Aranson, Flexibility of bacterial flagella in external shear results in complex swimming trajectories, *Journal of the Royal Society Interface*, **12** (2015), 1–11.
[21] A. Weil, *Elliptic Functions According to Eisenstein and Kronecker*, Springer-Verlag, 1976.

Received October 01, 2015; Accepted February 05, 2016.

E-mail address: czapla@up.krakow.pl
E-mail address: mityu@up.krakow.pl